Identification of emissive lanthanide complexes suitable for cellular imaging that resist quenching by endogenous anti-oxidants

Robert A. Poole,[a] Craig P. Montgomery,[a] Elizabeth J. New,[a] Aileen Congreve,[a] David Parker*[a] and Mauro Botta[b]

Received 19th April 2007, Accepted 14th May 2007
First published as an Advance Article on the web 31st May 2007
DOI: 10.1039/b705943d

Excited state quenching by urate and ascorbate of selected europium and terbium(III) macrocyclic complexes has been assessed and related to the ease of complex visualisation by optical microscopy inside various living cells, *e.g.* CHO, COS and NIH 3T3. It is the relative insensitivity of certain sterically encumbered complexes to dynamic quenching by urate that favours their usage for *in cellulo* applications. Non-covalent binding of the complex by protein also shields the excited lanthanide(III) ion from collisional quenching; this effect is most marked for a cationic triamide complex, $[Ln.\mathbf{1}]^{3+}$, consistent with its ease of visualisation by luminescence microscopy.

Introduction

Luminescent lanthanide complexes have been developed that can serve as 'tags' in bioconjugates for use in fluorescence resonance energy transfer (FRET) or tracking assays,[1,2] or as responsive probes.[3] Information about their local coordination environment or the concentration of a specific analyte in solution can be gained by monitoring changes in their spectral emission profile, lifetime or circular polarisation.[4] Recently, lanthanide complexes have been reported that are taken up by live cells and can be observed by fluorescence based microscopy techniques.[5–8] The intriguing possibility is emerging of using lanthanide complexes as *in cellulo* probes, reporting on a given biochemical parameter, *e.g.* enzyme activity, local pH, pM or pX.[3,9] The unique photophysical properties of lanthanide complexes, and the ease with which their structures can be modified to suit a particular application, can both complement and extend the 'tool kit' currently available for the analysis of living cells and the spatial and temporal profiles of certain processes that occur within them. Particular advantages over currently available fluorescent organic probes include their large Stokes shifts, long emission lifetimes (allowing time-resolved spectral or microscopic acquisition), insensitivity to dissolved oxygen and good chemical stability profile. In more recent work, the advantages of using ratiometric analyses have been highlighted, involving either monitoring a selection of two or more Eu emission bands[6,9] or examining two different lanthanide complexes of a common ligand. In the latter case, the differential sensitivity of the excited Eu and Tb(III) ions to dynamic quenching by urate has led to the development of a precise new assay for uric acid in biological fluids, such as diluted urine.[10]

The mechanism by which these complexes are able to cross the cell membrane and the factors that govern their localisation/compartmentalisation profile are not well understood. The structures of the lanthanide complexes [Ln.**1**]–[Ln.**6**] provide a cross-section of cyclen-based complexes that have been shown to be taken up by cells and to remain emissive once inside the cell.[3,6,7,9] In each case, the heterocyclic aromatic sensitising moiety is likely to serve a dual function. Not only may it serve as a sensitiser, but also it may be a key recognition element in binding to cell-surface or membrane bound proteins, hence, uptake/retention and endosome/vesicle recycling of the complexes may be a sensitive function of their differing protein affinity profiles. In the case of $[Ln.\mathbf{1}]^{3+}$, the tetraazatriphenylene moiety has earlier been shown to promote strong binding to *B*-DNA, so that the localisation of this cationic complex within the cell nucleus may at least be rationalised. For $[Tb.\mathbf{2}]^{+}$, the *o*-chlorophenylquinoline moiety reputedly targets benzodiazepine receptors that are over-expressed in glioblastoma cells[7]; some uptake studies have suggested that the complex may localise in the outer mitochondrial membrane, where the target receptors are expressed.

Unusual behaviour was exhibited by the constitutionally isomeric europium complexes $[Eu.\mathbf{3}]^{3+}$ and $[Eu.\mathbf{4}]^{3+}$: co-localisation studies with Lysotracker green showed that the former, and its zwitterionic and anionic analogues, localise in lysosomal compartments. In contrast, $[Eu.\mathbf{4}]^{3+}$ distributes quite well in the cytosol and there is some evidence to suggest that it stains the endoplasmic reticulum, following co-localisation studies with brefeldin A. The complexes $[Eu.\mathbf{5}]^{2-}$ and $[Eu.\mathbf{6}]^{3+}$ have been shown to cross the nuclear membrane and stain the nucleoli of mouse skin fibroblasts (NIH 3T3), Chinese hamster ovarian (CHO) and HeLa cells.[8a,9] In each of these structures there is a common azathiaxanthone moiety that is directly bound to the Eu ion. This rigid moiety must play a key role in reversible protein binding. This was demonstrated for each of these cases by the observation of relaxivity enhancements for the Gd analogues in the presence of serum albumin. Each complex, therefore, appears to bind to the RNA-protein adducts that are to be found in the ribosomes both inside the cell nucleus (in the dense and protein-rich regions of the nucleoli) and within the cytoplasm. Complexes $[Eu.\mathbf{2}]^{+}$ and $[Eu.\mathbf{3}]^{3+}$ are also most likely to enter the cell *via* an endocytotic pathway[11–15]; species that enter cells *via* endocytosis are believed to be initially trapped in endocytotic vesicles that are subsequently transferred into endosomes. Ageing endosomes

[a]*Department of Chemistry, Durham University, South Road, Durham, UK DH1 3LE. E-mail: david.parker@dur.ac.uk*
[b]*Dipartimento di Scienze dell'Ambiente e della Vita, Università del Piemonte Orientale "Amadeo Avogadro", Via Bellini 25/G, I-15100, Alessandria, Italy*

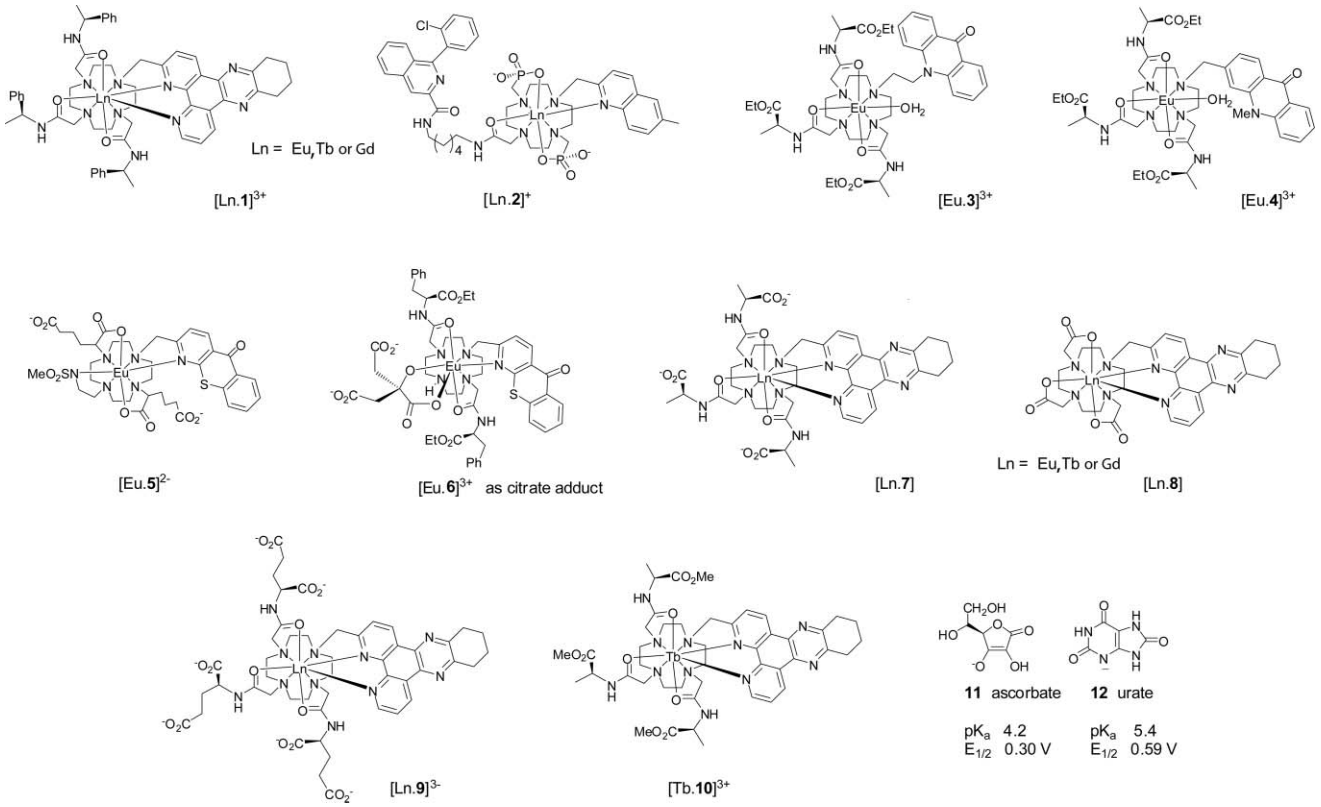

may transform into more acidic lysosomal compartments, that may become increasingly isolated from the rest of the cell. This is what appears to happen with [Eu.**2**]$^{+}$ and [Eu.**3**]$^{3+}$. If complexes taken up by this mechanism are to localise in other regions or compartments inside the cell, it is essential that they are able to escape from the pathway that leads to lysosomal formation.

Results and discussion

With this background in mind, a comparative analysis has been undertaken, using the neutral and anionic complexes [Ln.**7**], [Ln.**8**] and [Ln.**9**]$^{3-}$ (Ln = Tb or Eu) to assess the relative importance of charge and lipophilicity on the cellular uptake of the complexes, with [Ln.**1**]$^{3+}$ as a point of reference.[6c] In parallel, the sensitivity of each of these complexes to dynamic quenching of the lanthanide excited state has been assessed.

The anti-oxidants in the highest concentration within common cell types are ascorbate,**11**, and urate, **12**. Each is typically found in 0.2 mM concentration within cells, and preliminary work on their quenching ability has revealed that they are much more effective than glutathione (*ca.* 60 μM in cells) in quenching the lanthanide excited state by an electron or charge transfer process. A key issue is to relate the sensitivity of the 4 sets of complexes to quenching and compare this information to their ability to be observed by microscopy, within a common cell type.

Mouse skin fibroblast cells were cultured in DMEM (Dulbecco's Modified Eagle Medium) supplemented with 10% new-born calf serum, 50 g ml^{-1} penicillin and streptomycin, and non-essential amino acids, on 10 mm cover slips. When the confluence on the cover slip reached approximately 70%, the cells were loaded with an aqueous complex solution to give a final concentration in the growth medium of 1 mM. Following incubation for 24 hours, the cover glass to which the cells were attached was washed repeatedly with PBS (phosphate buffered saline) and placed onto a microscope slide (under these conditions [Ln.**1**]$^{3+}$ has been shown to localise within the cell nucleus).[5a,6c])

Each of the slides was imaged using a fluorescence microscope. Narrow excitation and emission filters were chosen (*excitation*: 345 nm low pass or Zeiss G365; *emission*: Eu 620 ± 25 nm or a 575–625 nm band pass, for Tb a 546 ± 25 nm band pass) such that the chromophore was irradiated at wavelengths corresponding only to its longest wavelength absorbance (*i.e.* centred at 348 nm) and the amount of scattered light reaching the CCD was minimised, to improve the signal to noise ratio. In capturing the images, it was apparent that considerably longer exposure times (by a factor of at least 4) were required to image luminescence from cells containing any of complexes [Ln.**7–9**], when compared to cells loaded with [Ln.**1**]$^{3+}$ under identical conditions. Even under these conditions, the signal to noise ratio was low and was only slightly above the level of background and scattered fluorescence, specific localisation was difficult to discern and there did not appear to be any evidence of nuclear localisation.

In order to provide a further example of a cationic complex against which complexes [Ln.**7–9**] could be compared, [Tb.**8**] was esterified at 20 °C in dry methanol in the presence of dry HCl to give the tri-positive methyl ester, [Tb.**10**]$^{3+}$ as its chloride salt. In contrast to the zwitterionic complex [Tb.**8**], it appeared to be taken up to a similar extent as [Ln.**1**]$^{3+}$, was readily observed and exhibited a similar cellular distribution. Typical localization profiles, revealed by time-resolved microscopy for [Eu.**1**]$^{3+}$ and [Tb.**1**]$^{3+}$ in CHO cells (3 h incubation, 50 μM complex in medium), are given in Fig. 1.

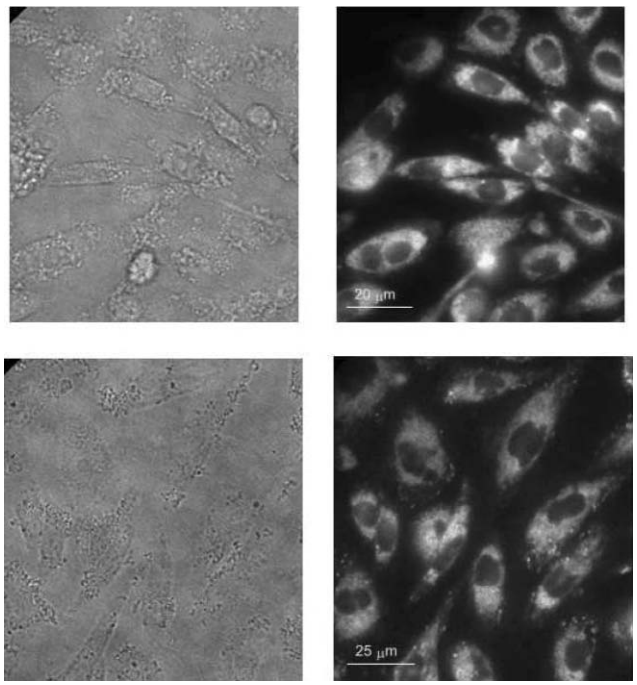

Fig. 1 Transmission (left) and luminescence microscope images (right) for CHO cells labelled with *upper*: $[Eu.\mathbf{1}]^{3+}$ (50 μM, 24 h post incubation) and *lower*, $[Tb.\mathbf{1}]^{3+}$ under the same conditions.

These results imply that either cellular uptake of the cationic complexes $[Ln.\mathbf{1}]^{3+}$ and $[Ln.\mathbf{10}]^{3+}$ is favoured compared to that of the related neutral and anionic complexes [Ln.**7–9**], or that the complexes may be taken up to a similar extent but emission from complexes [Ln.**7–9**] is more strongly quenched *in cellulo*. The local environment of the complex inside the cell is also not known but if, for example, the complexes were reversibly bound to protein (*e.g.* albumin) this too would affect their susceptibilities to dynamic quenching. In order to confirm the extent to which the complexes were taken up by the cells, an experiment was undertaken to determine the intracellular lanthanide concentration.

Intracellular concentration of selected europium complexes

The images obtained by fluorescence microscopy allow a comparison to be made between complexes in terms of their localisation or compartmentalisation profile within a cell. However, this does not provide quantitative information about how effectively the complexes are taken up. In order to quantify this, the concentration of each complex per cell was determined through a combination of flow-cytometry to determine the number of cells in a population, and ICP-MS (inductively coupled plasma mass spectrometry) which was used to determine the total lanthanide (europium) concentration. This approach was adopted by us earlier.[8a] Knowing the number of cells, the total number of moles of europium in the sample and an approximate volume for a cell, the concentration per cell can be determined. This allows a comparison to be drawn with the loading concentration. Alternatively, the number of moles of complex per cell can be quoted, eliminating the need to estimate the cell volume. Such an approach allows a comparison to be made between different cell lines.

The velocity of a cell as it passes through the flow chamber is in the order of 1 to 25 m s^{-1} (depending upon the operating pressure and nozzle diameter); the emissive lifetimes of the series of europium and terbium complexes are in the order of 1–2 ms. In conventional instruments, the laser intersection point is imaged to a pinhole located in front of the photomultiplier tube, as in confocal microscopy, this is done to eliminate out of focus light and scattered laser light from reaching the detector. However, due to the long emissive lifetimes of the lanthanide ions, only a small fraction of the total emission reaches the detector. Unless very high complex concentrations are used, this unfortunately renders them impractical as lumophores for cell sorting and counting. Time-resolved flow cytometers have been developed earlier for the measurement of lanthanide chelate fluorescence, but require modified instrumentation.[16] Emission is collected from the cell as it covers a distance of several millimetres passing through the flow chamber, corresponding to a time of the same order as the emissive lifetime of the complexes. A pinhole arrangement is not needed to prevent scattered light from reaching the detector since the laser is effectively 'off' during the acquisition period.

The complexes discussed here each incorporate a tetraazatriphenylene sensitising moiety. No fluorescence is observed from this chromophore either as a free species, or when it is coordinated to a lanthanide centre. Consequentially, it was necessary to find an alternative means through which the sample of cells could be labelled. This was achieved by dual labelling using the complex of interest and the acetylmethoxy ester of calcein (calcein AM). Calcein AM is a dye that is often used to assess cell viability in eukaryotic cells; in live cells, the non-fluorescent calcein AM is converted to green fluorescent calcein, following ester hydrolysis catalysed by intracellular esterases. It was therefore decided to co-localise CHO cells with both the lanthanide complex and calcein AM, allowing live cells containing the lanthanide complex to be selectively sorted and unviable cells discarded. As a control experiment, it was necessary to confirm that for a population of cells co-loaded with both calcein AM and complex, in every case where the green calcein emission could be observed, so too could lanthanide centred emission. CHO cells loaded with the europium complex [Eu.**1**] (50 μM, 3 hours incubation) and calcein AM (5 μM, 30 min incubation) were analysed by fluorescence microscopy using appropriate excitation and emission filters so that the red europium and green calcein emission could be examined separately. An additional advantage of the experiment was that it allowed an assessment of the viability of the cells to be made: only live cells contain the active esterase enzymes necessary to catalyse hydrolysis of the acetylmethoxy ester. It was found that for >97% of the cells examined, green and red emission could be observed simultaneously, thereby validating the flow cytometry method and providing evidence of the viability of the population of cells examined.

Populations of CHO cells were cultured to approximately 70% confluence in F-12 (Ham) growth medium, supplemented with 10% FBS (foetal bovine serum) and 50 mg ml^{-1} penicillin and streptomycin. Additions of europium complex and calcein AM were made as follows: CHO cells only—serving as a reference sample used to set up the flow cytometer, CHO cells + calcein AM (2 mM, 30 min incubation) used as a reference sample to set up detection parameters, CHO cells + complex (either $[Eu.\mathbf{1}]^{3+}$, [Eu.**8**] or $[Eu.\mathbf{9}]^{3-}$ = 50 or 100 μM, 3 h incubation) + calcein AM (5 μM, 30 min incubation).

Table 1 Concentrations (±10%) of Eu outside and inside the cell

Complex	Growth medium concentration[a]/μM	Intracellular concentration/μM
[Eu.**1**]$^{3+}$	49	26
[Eu.**8**]	31	12
[Eu.**9**]$^{3-}$	33	40

[a] Eu concentrations were determined by ICP-MS for CHO cells, values represent the concentration of Eu in the growth medium and within a cell by assuming a mean cell volume of 4000 μm^3.

Each of the cultures was washed 5 times with PBS to ensure that excess complex had been removed and was harvested using trypsin. The cells were collected by centrifugation and were re-suspended in buffer; the process was repeated 3 times. Each of the populations was finally suspended in 1 ml of phosphate buffer for introduction into the flow cytometer. Following successful sorting and collection, populations of cells co-loaded with both calcein and complex [Eu.**1**]$^{3+}$, [Eu.**8**] or [Eu.**9**]$^{3-}$ were recovered, containing a known number of cells. Typically, 20 000 to 100 000 cells were sorted and counted in this operation and the mean Eu concentrations in the growth medium and in the cells are listed in Table 1. Values reported in Table 1 show that each of the complexes is taken up to a similar extent by the cells; intracellular and extracellular concentrations also appear to be of the same magnitude. These results strongly suggest that it is the extent to which the complexes are quenched *in cellulo* that limits their utility as fluorescent probes, and not any uptake preference. The intracellular concentration estimated is an average across the whole cell and therefore the complex must be actively concentrated in certain compartments, in accordance with the punctuate nature of localisation.

Comparative analysis of complex sensitivity to quenching of the lanthanide excited state

The excited states of Eu(III) and Tb(III) ions lie 206 and 244 kJ mol^{-1} above the ground state and possess a radiative lifetime in the order of a millisecond. It is therefore not surprising that these relatively long-lived species are prone to quenching by collisional deactivation processes. Early work has highlighted the importance of dynamic quenching *via* electron transfer from common reductants. Ascorbate,**11**, and more particularly urate,**12**, have been shown to be effective in this regard.[6c,10] The quenching of the complexes [Ln.**1**]$^{3+}$, [Ln.**7**], [Ln.**8**] and [Ln.**9**]$^{3-}$ by urate and ascorbate was therefore studied at pH 7.4 [0.1 M 4-(2-hydroxyethyl)-1-piperazineethanesulfonic acid (HEPES), 10 mM NaCl, 298 K]. Variations in emission lifetime echoed the changes measured in the lifetime of the excited state, consistent with a dynamic collisional deactivation mechanism. Such behaviour is commonly discussed in terms of a Stern–Volmer analysis, in which the Stern–Volmer quenching constants ($1/K_{SV}$ in mM) and the second-order rate constant, k_q, reflect the sensitivity of the excited state to quenching, eqn (1). The term τ_0 is the excited state lifetime in the absence of added quencher, Q.

$$\tau_0/\tau = 1 + k_q\tau_0[Q] = 1 + K_{SV}[Q] \quad (1)$$

Examining the results summarized in Table 2, several conclusions may be drawn. In each case, the terbium complexes are quenched considerably more strongly than their europium analogues; this behaviour is consistent with a mechanism in which it is the excited state energy of the lanthanide that drives the quenching process, *viz.* the higher free energy of the terbium $^5D_4$ state. It might be expected that the quenching ability of urate and ascorbate would reflect their one electron oxidation potentials (0.59 and 0.30 V respectively).[17,18] This is certainly not the case here, and urate is 20 to 50 times more effective than ascorbate in quenching [Ln.**8**] and [Ln.**9**]$^{3-}$, as pointed out earlier.[10] Moreover, the charge neutral and anionic complexes are quenched less by ascorbate than the cationic complex, in line with Coulombic attraction, however, such a trend is not followed for urate quenching. For example, in the case of the most quenched complex, [Tb.**8**], $k_q = 1.8 \times 10^8$ M^{-1} s^{-1}, a value three times higher than for the anionic and cationic examples.

Table 2 Quenching parameters[a,b,c] for selected lanthanide complexes towards urate and ascorbate (parentheses)

Complex	K_{SV}^{-1}/mM	$k_q \times 10^7$/M^{-1} s^{-1}	τ_o/τ
[Eu.**1**]$^{3+}$	0.07 (0.39)	1.4 (0.25)	1.7[d]
[Tb.**1**]$^{3+}$	0.017 (0.18)	6.0 (0.66)	5.1[d]
[Eu.**7**]	0.05 (1.13)	2.0 (0.09)	2
[Tb.**7**]	0.05 (0.55)	2.0 (0.18)	2.2
[Eu.**8**]	0.11 (2.43)	0.86 (0.04)	1.4
[Tb.**8**]	0.005 (0.30)	18 (0.35)	11.6
[Eu.**9**]$^{3-}$	0.084 (2.55)	1.1 (0.035)	1.6
[Tb.**9**]$^{3-}$	0.011 (0.38)	5.7 (0.18)	5.6

[a] τ_o/τ values are given for 50 μM added quencher, corresponding to putative intracellular quencher concentrations. [b] The most well-defined 'linear' range for the observed dynamic quenching was typically 10–50 μM for urate and 100–500 μM for ascorbate quenching, when the complex concentration was 10 μM (pH 7.4, 10 mM NaCl, 100 mM HEPES, 295 K). [c] For ascorbate, τ_o/τ values for 50 μM added quencher remain near unity ($\leq$ 1.2 in each case); at 0.2 mM ascorbate the τ_o/τ value is $\leq$ 2 (±0.5) for each of the above complexes (and near unity for [Eu.**8**] and [Eu.**9**]$^{3-}$). [d] Non-linear plots were obtained.

The Stern–Volmer plots generally have a constant gradient, *i.e.* behave ideally, but the range of quencher concentrations was selected carefully; above a certain value the rate of change of τ_0/τ *versus* concentration of quencher decreases and curvature is apparent in the Stern–Volmer plot, *i.e.* a limiting value is reached (Fig. 2). As a result, the range of concentrations of a given quencher had to be carefully chosen, in order for ideal Stern–Volmer behaviour to be observed. The ranges used were 0.1–0.5 mM for ascorbate but only 10–50 μM for urate (the complex was used at a concentration of 10 μM). However, the point at which this limit was reached with a given quenching species was dependent upon the complex under study. For example, for quenching of [Ln.**1**]$^{3+}$ with urate, it was apparent that a limiting lifetime is reached at a fairly low urate concentration and curvature was apparent in their Stern–Volmer plots in the range 50–200 μM. For the neutral and anionic complexes [Ln.**8**] and [Ln.**9**]$^{3-}$ concentrations at least 3 to 5 times as high were

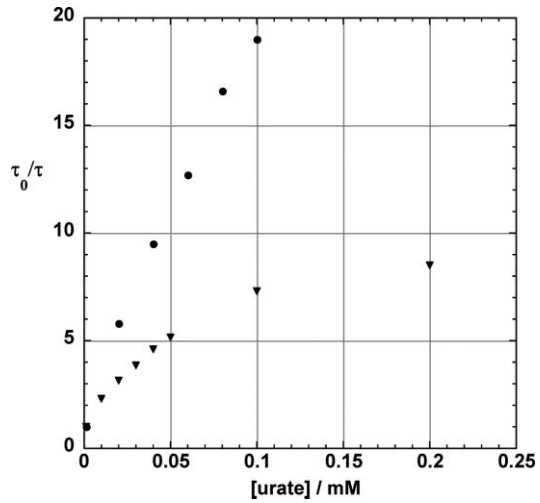

Fig. 2 Stern–Volmer plot showing the variation in τ_o/τ for [Tb.**1**]$(CF_3SO_3)_3$ (▼) and [Tb.**8**] (●) with increasing amounts of added urate (298 K, pH 7.4, 0.1M HEPES).

required before their Stern–Volmer plots became non-linear. A way of quantifying this effect is to compare the measured τ_0/τ values for a fixed concentration (here taken as 50 μM, Table 2) of added urate: values were 11.6 for [Tb.**8**], 5.6 for [Tb.**9**]$^{3-}$ and 5.1 for [Tb.**1**]$^{3+}$.

Consideration of the structures of ascorbate and urate, **11** and **12**, and how they might interact with each of the complexes can perhaps help to provide some insight into the quenching mechanism. The urate mono-anion (pK_a 5.4) has a 2-dimensional structure with an electron-rich π system in which charge is delocalized onto N-3, N-7 and the two amide oxygens.[19,20] Ascorbate (pK_a 4.2), in contrast, has a less conjugated π-system and is significantly more hydrophilic, with a much higher limiting solubility in water (approximately 2 M *vs.* 5 mM for urate).

There are two mechanisms that have been promulgated to represent the kinetics of excited state electron transfer; the first was proposed by Rehm and Weller[21,22] and involves reversible formation of an encounter complex, followed by electron transfer between the donor (D = Q) and the acceptor, A, Scheme 1. The kinetic analysis of this scheme (ignoring non-radiative decay processes) follows classical Stern–Volmer behaviour, eqn (1).

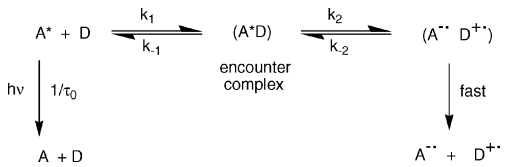

Scheme 1

It is plausible that quenching could be promoted in the case of urate by a weak but favourable binding interaction, involving π-stacking between the electron poor tetraazatriphenylene moiety and urate. This binding interaction allows an alternative quenching mechanism to be considered, leading to similar overall competitive kinetics.

It has been reported by several authors that for planar aromatic donor–acceptor pairs, quenching may be associated with formation of an exciplex rather than through formation of radical–ion

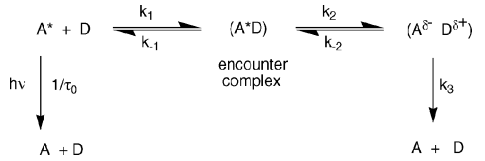

Scheme 2

pairs, Scheme 2;[23,24] the exciplex lifetime is $1/k_3$. In this case, the term K_{SV} has a completely different sense and should be considered as an equilibrium constant associated with reversible exciplex formation, $K_{ex} = k_1k_2/k_{-1}k_{-2}$, provided that $k_{-2} \gg k_3$. Under these circumstances, the observed lifetime τ of the emissive lanthanide, being in equilibrium with the exciplex, will vary with the quencher concentration in a non-linear manner, eqn 2. The plot of τ_o/τ *versus* quencher concentration, [Q], then has an initial slope different to the apparent Stern–Volmer constant, and may reach a limit equal to $\tau_o k_3$ at higher quencher concentrations.[23]

$$\tau_0/\tau = (1 + k_3\tau_0K_{ex}[Q])/(1 + K_{ex}[Q]) \quad (2)$$

The neutral complexes [Ln.**7**] and [Ln.**8**], have less steric crowding around the Ln ion and have a more sterically accessible chromophore, hence, they may be expected to be the most strongly quenched where such interactions are possible. The cationic complex [Ln.**1**]$^{3+}$, in contrast, notwithstanding a favourable Coulombic interaction with urate/ascorbate, is more sterically crowded around the Ln ion, and has a lower solvent-accessible surface area; any π-stacking interaction with the diffusing urate anion is likely to be somewhat inhibited.

These observations appear to suggest that limits are reached at lower added quencher concentrations, when there is the possibility of some favourable association between the complex and the quenching species. This could be through a weak hydrogen-bonding interaction with ascorbate, or more notably for urate, it may occur *via* an attractive charge transfer or π–π attraction with the electron poor tetraazatriphenylene chromophore. The onset of non-linearity in the Stern–Volmer plot may also reflect the point at which k_q[Q] is close in magnitude to k_{em}, *i.e.* where the rate of quenching of the lanthanide excited state is comparable to the rate of decay of the observed emission. Indeed, the emission decay profiles in this 'non-linear' region did not correspond to a simple mono-exponential decay. Therefore, when an apparent lifetime was estimated in this region, the lifetime was estimated by analyzing the first 25 to 35% of the observed decay curve.

Effect of protein binding on sensitivity to quenching

Protein is present in the cell growth medium and within the cell. It was thought that if the complexes exhibited an affinity towards protein, then uptake of the complex would be affected, indeed, uptake may be protein mediated. In addition, if a complex is protein bound, it may be expected to display a different sensitivity to collisional quenching. The gadolinium complexes, [Gd.**1**]$^{3+}$ and [Gd.**8**] were examined first in order to assess their affinity for protein binding. Extensive studies on the field and T dependence of the proton relaxivity (the increment of the water proton relaxation rate per unit concentration) of Gd complexes in the presence of protein have revealed certain key characteristics.[25] Protein binding is predicted to give both complexes an increase in relaxivity at all field strengths, even for systems that lack a bound water molecule.[26]

There is also a change in the form of the field dependence of relaxivity (an NMRD profile) for protein bound species, with a minimum around 1–10 MHz and a maximum in the range 20–60 MHz, where the rotational correlation term, τ_r, associated with the reorientation of the Gd–water vector, primarily determines the measured relaxivity.

The relaxivities of [Gd.**1**]$^{3+}$ and [Gd.**8**] were measured to be 2.5 and 2.2 mM^{-1} s^{-1} respectively (310 K, 60 MHz). These are typical values for Gd complexes of this molecular volume that lack a metal bound water molecule (*i.e.* $q = 0$). In the presence of 0.4 mM added serum albumin, the relaxivity of [Gd.**1**]$^{3+}$ increased by a factor of more than two in the range 0.001–1 MHz, exhibited a change in form and a large increase at higher field, with a maximum around 30 MHz (Fig. 3). This NMRD profile is typical of a protein bound complex in which there are a few second-sphere water molecules that are relatively tightly bound to the complex.[25] Although detailed fitting analyses have not been undertaken, the form of the profile may be interpreted in terms of a complex that exhibits both a long τ_r and a relatively long water exchange lifetime, τ_m, for the second-sphere waters. Observed relaxivities are relatively high in the presence of protein, for a $q = 0$ system.

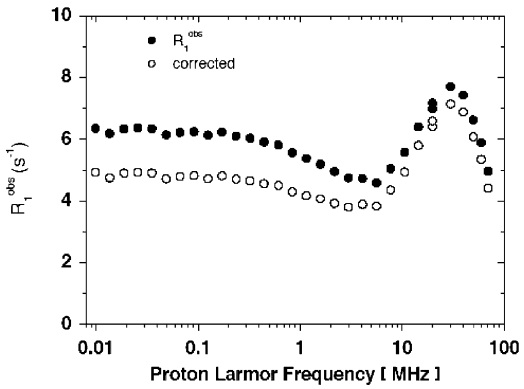

Fig. 3 NMRD plot showing the variation in the measured water proton longitudinal relaxation rate, R_1, with applied field for [Gd.**1**]Cl_3 (0.4 mM) in the presence of added human serum albumin (0.4 mM, 298 K); the data in open circles are corrected for the effect of the added protein.

The relaxivity of [Gd.**1**]$^{3+}$ (1.7 mM in this analysis) was measured as a function of added human serum albumin at 37 °C at 60 MHz (Fig. 4). The binding constant for coordination of the complex to HSA could not be estimated accurately as the stoichiometry of

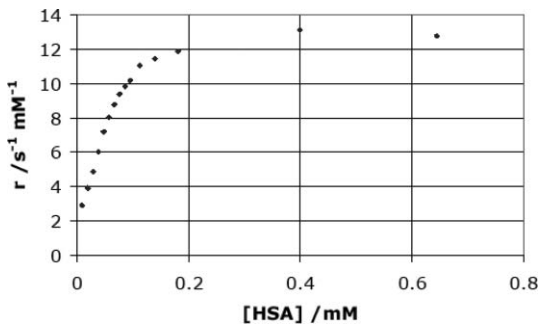

Fig. 4 Variation of the proton relaxivity (310 K, 60 MHz) of [Gd.**1**]Cl_3 (1.6 mM) with added human serum albumin, showing a relaxivity enhancement associated with non-specific binding of the complex to the protein.

complexation is not easily determined. However, the large increase in relaxivity confirms that the binding affinity is high. An upper limit is reached at a ratio of approximately 8 to 10 complex molecules per protein (as observed for [Gd.**6**]$^{3+}$),[8a] suggesting a non-specific binding mode and precluding a binding mechanism involving incorporation of the complex into a specific albumin binding pocket, as is commonly found for a range of lipophilic, anionic Gd complexes, *e.g.* [Gd.**5**]$^{2-}$.[9,25,27,28] Given that the concentration of protein within the cell is likely to be >0.2 mM, the cationic complex is likely to be >90% protein bound. For [Gd.**8**], protein binding caused a much smaller enhancement in relaxivity. After addition of 0.1 and 0.4 mM to an 0.6 mM solution of [Gd.**8**] (37 °C, 60 MHz), only an 8 and 16% increase in measured relaxivity was observed, consistent with a very weak protein affinity.

The sensitivity of [Tb.**1**]$^{3+}$ and [Tb.**8**] to excited state quenching by urate was assessed in the presence of 0.4 mM serum albumin, measuring the τ_o/τ values at 10, 50 and 100 μM added urate. For [Tb.**1**]$^{3+}$ the presence of added protein clearly rendered the complex less sensitive to dynamic quenching: measured τ_o/τ values at 10, 50 and 100 μM added urate were 1.03, 1.19 and 1.36 compared to 1.63, 3.59 and 5.24 in the absence of protein. For [Gd.**8**], corresponding τ_o/τ values were 2.41, 6.38 and 7.39 compared to 3.31, 9.88 and 14.7 in the absence of protein.

In a control experiment, the quenching effect of added protein was also examined, by observing the change in the Tb emission lifetime as a function of added protein, over the protein concentration range 0 to 0.7 mM. Plots of τ_o/τ as a function of the concentration of added protein showed that for [Tb.**1**]$^{3+}$, a limiting τ_o/τ value of 1.36 was reached following addition of 0.15 mM serum albumin, with a limiting lifetime of 0.62 ms. With [Tb.**8**], on the other hand, τ_o/τ increased almost linearly as a function of added protein: $\tau_o/\tau = 1.4$ for 0.2 mM added protein and $\tau_o/\tau = 1.77$ at 0.4 mM protein. The differing behaviour of the two complexes is in line with the differing protein affinities deduced from the relaxivity measurements made on the Gd analogues.

The measured lifetimes for [Tb.**1**]$^{3+}$ and [Tb.**8**] (0.1 mM) in the presence of 0.1 mM urate and 0.4 mM serum albumin were 0.57 and 0.06 ms respectively (298 K). Evidently, protein association of the cationic complex shields the Tb(III) ion from urate quenching. With [Tb.**8**], protein binding inhibits, but does not suppress, urate quenching. Hence, the cationic complex is an order of magnitude more long-lived, and hence more emissive, with protein and urate present. The cationic complex is therefore more likely to be significantly more emissive, when localized within the cell.

Preliminary analysis of intracellular complex emissive lifetimes

Through the use of a time-resolved microscope, it is possible to determine the lifetime at any point within an image, with appropriate treatment, a lifetime 'density' map can be built up.[29] Quenching of the lanthanide excited state is characterised by a decrease in the metal centred emission lifetime, in addition to a decrease in emission intensity. This method provides a useful technique for probing the local environment of the complex.

Chinese hamster ovarian (CHO) cells were incubated in the presence of a 1 mM solution containing [Eu.**1**]$^{3+}$ for 4 h, under conditions which have been shown previously to lead to intranuclear localisation. Images were then captured using gate times of between 0 and 2500 ms in 125 ms steps following excitation using

a nitrogen laser at 337 nm. By plotting the change in emission intensity for individual pixels, or over a region of interest as a function of gate time, it was possible to estimate the lifetime of the complex over that area. This principle was examined for a region of interest centred on the punctuate localisation around the periphery of the nucleus and for another region centred inside the cell nucleus. Lifetimes were found to be 716 ms and 769 ms over each region, respectively. Whilst these are preliminary results, it is interesting to note that the lifetimes are relatively long (*cf.* 1 ms for the complex in water), indicating that [Eu.**1**]$^{3+}$ is not strongly quenched within the cell. Following optimisation of the method, it would be interesting to compare lifetime mapping studies for those complexes that appear to give only very weak emission *in cellulo*. The results of such studies will be reported in subsequent articles, using a more sensitive time-resolved microscopy facility, being constructed in Durham.

Summary and conclusions

The sensitivity of europium and terbium(III) macrocyclic complexes to dynamic quenching of their excited state is a key factor in defining their utility as probes for intracellular usage. It is the relative insensitivity of more sterically encumbered complexes, *e.g.* [Ln.**1**]$^{3+}$, to dynamic quenching by urate that favours its usage for *in cellulo* applications. These complexes typically possess a heterocyclic moiety that can aid binding to albumin; such reversible non-covalent binding of the complex by protein also shields the excited lanthanide(III) ion from collisional quenching. The effect is most marked for the cationic triamide complex, [Ln.**1**]$^{3+}$, consistent with its ease of visualisation by luminescence microscopy. Future probe development should therefore pay due deference to these issues, otherwise the complex may be difficult to observe by luminescence microscopy.

Experimental

Lifetime measurements were measured by excitation of the sample by a short pulse of light (348 nm) followed by monitoring the integrated intensity of light (545 nm for terbium, 620 nm for europium) emitted during a fixed gate time, t_g, a delay time, t_d, later. At least 20 delay times were used covering 3 or more lifetimes. A gate time of 0.1 ms was used, and the excitation and emission slits were set to 10 and 2.5 nm band pass respectively. The obtained decay curves were fitted to the equation below using Microsoft Excel.

$$I = A_0 + A_1\exp(-kt)$$

where I = intensity at time t after the flash, A_0 = intensity after the decay has finished, A_1 = pre-exponential factor, k = rate constant for decay of the excited state. The excited state lifetime, τ, is the inverse of the rate constant, k.

Epifluorescence images were taken on a Zeiss Axiovert 200 M epifluorescence microscope with a digital camera, or a custom, time-resolved fluorescence microscope using nitrogen laser excitation at 337 nm; confocal images were taken on a Zeiss LSM 500 META confocal microscope with 405 nm diode laser excitation and an LP 505 emission filter for europium complex luminescence and with 488 nm argon laser excitation and a BP 505–550 filter for SYTO dye fluorescence.

Flow cytometric analysis and sorting was conducted using a DakoCytomation Inc. MoFlo multi-laser flow cytometer (Fort Collins, CO, USA) operating at 60 psi, 70 micron nozzle. Samples were interrogated with a 100 mW, 488 nm solid state laser (FSC, SSC). Fluorescence signals were detected and collected through the FL1 (530/40) interference filter in logarithmic mode. The data were analyzed using Summit v4.3 (DakoCytomation) software.[30]

Inductively coupled plasma mass spectrometry determination of europium concentrations was made following dilution of the sample in dilute nitric acid. Relaxivity measurements were made at 37 °C and 60 MHz on a Bruker Minispec mq60 instrument. The mean value of three separate measurements was recorded. NMRD profiles were recorded in Durham on a Stelar Spinmaster, in the field range 0.001–20 MHz and in Ivrea, Italy on a similar instrument operating up to 70 MHz.

Cell culture and complex loading

NIH 3T3, CHO or COS cells were incubated under 5% carbon dioxide–air at 37 °C, in DMEM with 4.5 g L^{-1} glucose, L-glutamine and pyruvate, supplemented with 10% natal bovine serum and a 1% penicillin–streptomycin mixture. For microscopy, cells seeded on cover-slips were incubated with the complex dissolved in fresh medium at 37 °C or 4 °C in a 12-well plate for the indicated time. The cells were washed with PBS (phosphate buffered saline) at least 5 times, and mounted onto slides for measurement. For luminescence spectral measurement, the cells were incubated in a 100 mm Petri dish with the complex and washed with PBS at least 5 times, then harvested with 1 mL of trypsin [0.25% (w/v)]. The mixture was diluted to 10 mL with PBS and centrifuged. The precipitates were collected and re-suspended in PBS to 1.5 mL for spectral measurements. The cover-slips were then washed with PBS at least 8 times and mounted onto slides for microscopy.

Cell viability studies were carried out by loading either the NIH 3T3 or CHO cells with complex (100 μM, 4 h) or with calcein AM (5 μM, 30 min) and separately with both complex and dye. The cells were handled in a 12-well plate and were washed with PBS and mounted onto slides for examination as described above. Cells were examined by microscopy using the appropriate excitation and emission filters, so that the red europium emission and green calcein fluorescence could be distinguished separately. For the co-loaded cells, emission was observed for >97% of the cells examined, corresponding to both the complex and the dye, consistent with good cell viability.

Acknowledgements

We thank the Association of Commonwealth Universities for a Scholarship (EJN), CISbio s.a. (CM), EPSRC (RAP, AC) and the Royal Society (DP) for support. Epifluorescence images were obtained with the assistance of Michel Laget (Cisbio International, France). ICP-MS determinations were made by Dr C. Ottley in the Department of Earth Sciences at Durham University.

References

1 H. Bazin, E. Trinquet and G. Mathis, *Rev. Mol. Biotechnol.*, 2002, **82**, 233.
2 P. R. Selvin, *Annu. Rev. Biophys. Biomol. Struct.*, 2002, **31**, 275; I. Hemmila and V.-M. Mukkala, *Crit. Rev. Clin. Lab. Sci.*, 2001, **38**, 441.

3 S. Pandya, J. Yu and D. Parker, *Dalton Trans.*, 2006, 2757; T. Gunnlaugsson, D. Parker and O. Reany, *Chem. Commun.*, 2000, 473; O. Reany, D. Parker and T. Gunnlaugsson, *J. Chem. Soc., Perkin Trans. 2*, 2000, 1819; B. Song, E. Wong and J. Yuan, *Chem. Commun.*, 2005, 3553; D. Parker and J. A. G. Williams, *Chem. Commun.*, 1998, 245; T. Terai, K. Kikuchi, S. Y. Isawasa, T. Kawabe, Y. Hirata, Y. Urano and T. Nagano, *J. Am. Chem. Soc.*, 2006, **128**, 6938.
4 D. Parker, *Coord. Chem. Rev.*, 2000, **205**, 109; R. S. Dickins, D. Parker, C. Crossland, J. A. K. Howard and H. Puschmann, *Chem. Rev.*, 2002, **102**, 1977; R. S. Dickins, J. A. K. Howard, J. M. Moloney, D. Parker and R. D. Peacock, *Angew. Chem., Int. Ed. Engl.*, 1997, **36**, 521; S. Petoud, G. Muller, E. G. Moore, J. D. Xu, J. Sokolnicki, J. P. Riehl, U. N. Le, S. M. Cohen and K. N. Raymond, *J. Am. Chem. Soc.*, 2007, **129**, 77; P. Atkinson, Y. Bretonniere, G. Muller and D. Parker, *Helv. Chim. Acta*, 2005, **88**, 391.
5 (*a*) J.-C. Frias, G. Bobba, M. J. Cann, D. Parker and C. J. Hutchison, *Org. Biomol. Chem.*, 2003, **1**, 905; (*b*) G. Bobba, J.-C. Frias and D. Parker, *Chem. Commun.*, 2002, 890.
6 (*a*) Y. Brettoniere, M. J. Cann, D. Parker and R. Slater, *Chem. Commun.*, 2002, 1930; (*b*) Y. Brettoniere, M. J. Cann, D. Parker and R. Slater, *Org. Biomol. Chem.*, 2004, **2**, 1624; (*c*) R. A. Poole, G. Bobba, M. J. Cann, J.-C. Frias, D. Parker and R. D. Peacock, *Org. Biomol. Chem.*, 2005, **3**, 1013; (*d*) A.-S. Chauvin, C. Vandevyver, S. Comby and J.-C. G. Bunzli, *Chem. Commun.*, 2007, 1716.
7 H. C. Manning, T. Goebel, R. C. Thompson, R. R. Price, H. Lee and D. J. Bornhop, *Bioconjugate Chem.*, 2004, **15**, 1488; D. J. Bornhop, J. M. M. Griffin, T. S. Goebel, M. R. Sudduth, B. Bell and M. Motamedi, *Appl. Spectrosc.*, 2003, **57**, 1216.
8 (*a*) J. Yu, D. Parker, R. Pal, R. A. Poole and M. J. Cann, *J. Am. Chem. Soc.*, 2006, **128**, 2294; (*b*) K. Hanoaka, K. Kikuchi, H. Kojima, Y. Urano and T. Nagano, *J. Am. Chem. Soc.*, 2004, **126**, 12470.
9 R. Pal and D. Parker, *Chem. Commun.*, 2007, 474.
10 R. A. Poole, F. Kielar, S. L. Richardson, P. A. Stenson and D. Parker, *Chem. Commun.*, 2006, 4084.
11 N. A. Campbell, J. B. Reece and L. G. Mitchell, *Biology*, Addison Wesley Longman, New York, 5th edn, 1999.
12 I. Mellman, *Annu. Rev. Cell Dev. Biol.*, 1996, **12**, 575.
13 C. Schnatwinkel, S. Chrisforidis, M. R. Lindsay, S. Uttenweiler-Joseph and M. Wilm, *PLoS Biol.*, 2004, **2**(9), 1249.
14 B. J. Nichols and J. Lippincott-Schwartz, *Trends Cell Biol.*, 2001, **11**(10), 406.
15 L. Pelkmans and A. Helenius, *Traffic*, 2002, **3**, 311.
16 M. A. Condrau, R. A. Schwender, M. Zimmermann, M. H. Muser, U. Graf, P. Niederer and M. Anliker, *Cytometry*, 1994, **16**, 195.
17 S. Steenken and P. Neta, *J. Phys. Chem.*, 1982, **86**, 3661; S. Steenken and P. Neta, *J. Phys. Chem.*, 1979, **83**, 1134.
18 M. G. Simic and S. V. Jovanovic, *J. Am. Chem. Soc.*, 1989, **111**, 5778.
19 N. S. Mandel and G. S. Mandel, *J. Am. Chem. Soc.*, 1976, **98**, 2319.
20 J. P. Telo, *Org. Biomol. Chem.*, 2003, **1**, 588.
21 D. Rehm and A. Weller, *Ber. Bunsen-Ges.*, 1969, **73**, 834.
22 D. Rehm and A. Weller, *Isr. J. Chem.*, 1970, **8**, 259.
23 M. G. Kuzmin, *Pure Appl. Chem.*, 1993, **65**, 1653.
24 M. Dossot, D. Burget, X. Allonas and P. Jacques, *New J. Chem.*, 2001, **25**, 194.
25 P. Caravan, J. J. Ellison, T. J. McMurry and R. B. Lauffer, *Chem. Rev.*, 1999, **99**, 2293.
26 S. Aime, A. S. Batsanov, M. Botta, J. A. K. Howard, D. Parker, P. K. Senanayake and J. A. G. Williams, *Inorg. Chem.*, 1994, **33**, 4696.
27 P. Caravan, N. J. Cloutier, M. T. Greenfield, S. A. McDermid, S. U. Dunham, J. W. M. Bulte, J. C. Amedio, Jr., R. J. Looby, R. P. Supkowski, W. deW. Horrocks, Jr., T. J. McMurry and R. B. Lauffer, *J. Am. Chem. Soc.*, 2002, **124**(12), 3152.
28 S. Aime, A. Barge, M. Botta and E. Terreno, in *Metal Ions in Biological Systems*, ed. H. Sigel and A. Sigel, Marcel Dekker Inc., New York, vol. 40, p. 643.
29 A. Beeby, S. Botchway, I. M. Clarkson, S. Faulkner, A. W. Parker, D. Parker and J. A. G. Williams, *J. Photochem. Photobiol., B*, 2000, **57**, 83.
30 S. W. Parsley, Dako Corporation, Fort Collins, Colorado, 2006.

